Modeling glacier thickness distribution and bed topography over entire mountain ranges with GlabTop: Application of a fast and robust approach

Linsbauer, Andreas ; Paul, Frank ; Haeberli, Wilfried

Abstract: The combination of glacier outlines with digital elevation models (DEMs) opens new dimensions for research on climate change impacts over entire mountain chains. Of particular interest is the modeling of glacier thickness distribution, where several new approaches were proposed recently. The tool applied herein, GlabTop (Glacier bed Topography) is a fast and robust approach to model thickness distribution and bed topography for large glacier samples using a Geographic Information System (GIS). The method is based on an empirical relation between average basal shear stress and elevation range of individual glaciers, calibrated with geometric information from paleoglaciers, and validated with radio echo soundings on contemporary glaciers. It represents an alternative and independent test possibility for approaches based on mass-conservation and flow. As an example for using GlabTop in entire mountain ranges, we here present the modeled ice thickness distribution and bed topography for all Swiss glaciers along with a geomorphometric analysis of glacier characteristics and the overdeepenings found in the modeled glacier bed. These overdeepenings can be seen as potential sites for future lake formation and are thus highly relevant in connection with hydropower production and natural hazards. The thickest ice of the largest glaciers rests on weakly inclined bedrock at comparably low elevations, resulting in a limited potential for a terminus retreat to higher elevations. The calculated total glacier volume for all Swiss glaciers is 75 ± 22 km3 for 1973 and 65 ± 20 km3 in 1999. Considering an uncertainty range of ±30%, these results are in good agreement with estimates from other approaches.

DOI: https://doi.org/10.1029/2011JF002313

Modeling glacier thickness distribution and bed topography over entire mountain ranges with GlabTop: Application of a fast and robust approach

A. Linsbauer,[1] F. Paul,[1] and W. Haeberli[1]

Received 23 December 2011; revised 16 May 2012; accepted 27 May 2012; published 31 July 2012.

[1] The combination of glacier outlines with digital elevation models (DEMs) opens new dimensions for research on climate change impacts over entire mountain chains. Of particular interest is the modeling of glacier thickness distribution, where several new approaches were proposed recently. The tool applied herein, GlabTop (Glacier bed Topography) is a fast and robust approach to model thickness distribution and bed topography for large glacier samples using a Geographic Information System (GIS). The method is based on an empirical relation between average basal shear stress and elevation range of individual glaciers, calibrated with geometric information from paleoglaciers, and validated with radio echo soundings on contemporary glaciers. It represents an alternative and independent test possibility for approaches based on mass-conservation and flow. As an example for using GlabTop in entire mountain ranges, we here present the modeled ice thickness distribution and bed topography for all Swiss glaciers along with a geomorphometric analysis of glacier characteristics and the overdeepenings found in the modeled glacier bed. These overdeepenings can be seen as potential sites for future lake formation and are thus highly relevant in connection with hydropower production and natural hazards. The thickest ice of the largest glaciers rests on weakly inclined bedrock at comparably low elevations, resulting in a limited potential for a terminus retreat to higher elevations. The calculated total glacier volume for all Swiss glaciers is 75 ± 22 km^3 for 1973 and 65 ± 20 km^3 in 1999. Considering an uncertainty range of $\pm 30\%$, these results are in good agreement with estimates from other approaches.

Citation: Linsbauer, A., F. Paul, and W. Haeberli (2012), Modeling glacier thickness distribution and bed topography over entire mountain ranges with GlabTop: Application of a fast and robust approach, *J. Geophys. Res.*, *117*, F03007, doi:10.1029/2011JF002313.

1. Introduction

[2] The ongoing increase in global mean temperature has caused substantial decline for most glaciers in the world [*World Glacier Monitoring Service* (*WGMS*), 2008; *Lemke et al.*, 2007; *Watson and Haeberli*, 2004]. Accelerated glacier loss in high-mountain regions, [e.g., *Paul et al.*, 2007a] can have strong environmental as well as economic impacts at local to regional and even continental to global scales (hydro-power, water resources, sea level rise [e.g., *Zemp et al.*, 2007; *WGMS*, 2008]). When observed glacier changes are combined with digitized glacier inventories and digital elevation models (DEMs), an important knowledge basis for timely anticipation and quantitative modeling of such changes is at hand [e.g., *Huss et al.*, 2010; *Künzler et al.*, 2010; *Paul et al.*, 2007b]. A most prominent application of the combined data sets is the modeling of the ice thickness distribution for larger samples of glaciers from simplified glaciological principles [e.g., *Paul and Linsbauer*, 2012; *Li et al.*, 2012, 2011; *Farinotti et al.*, 2009b; *Clarke et al.*, 2009]. Beside the improved calculation of glacier volume that is an urgent demand also on a global scale [*Radic and Hock*, 2010], a further simple step is the subtraction of the modeled ice thickness from a surface DEM providing a DEM without glaciers, i.e., an approximation of the subglacial topography [e.g., *Linsbauer et al.*, 2009; *Binder et al.*, 2009]. This type of information is important for the modeling of future glacier evolution according to given climate change scenarios [e.g., *Jouvet et al.*, 2009, 2011]. The calculated glacier bed further allows assessment of related impacts, for example on changing runoff regimes [*Huss et al.*, 2010], the potential formation of new lakes in subglacial depressions or of future hazard conditions [*Frey et al.*, 2010; *Künzler et al.*, 2010; *Quincey et al.*, 2007; *Rothenbühler*, 2006]. There are still high uncertainties involved in all methods used for

[1]Department of Geography, University of Zurich, Zurich, Switzerland.

Corresponding author: A. Linsbauer, Department of Geography, University of Zurich, Winterthurerstr. 190, CH-8057 Zurich, Switzerland. (andreas.linsbauer@geo.uzh.ch)

0148-0227/12/2011JF002313

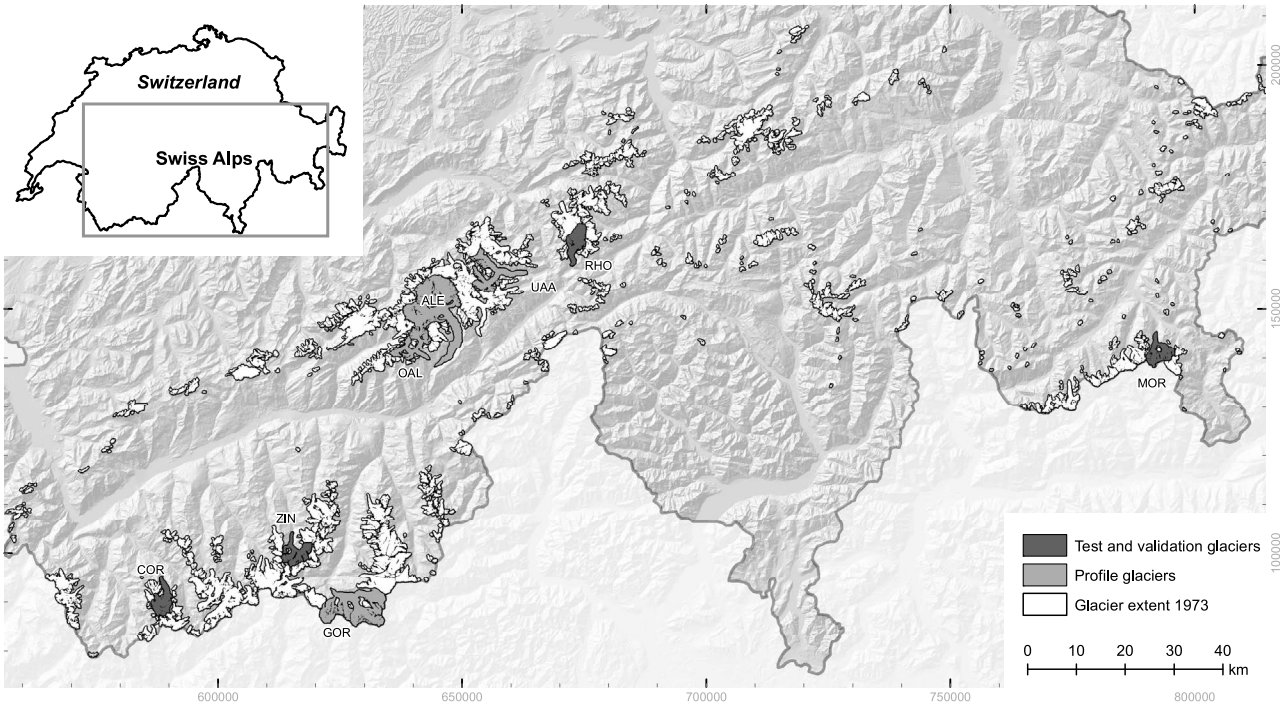

Figure 1. Model domain showing all Swiss glacier with their extend from 1973. Abbreviations refer to the following glaciers: MOR, Morteratsch; RHO, Rhone; UAA, Unteraar; ALE, Great Aletsch; OAL, Oberaletsch; GOR, Gorner; ZIN, Zinal; COR, Corbassière.

estimating glacier thickness, but even approximately reconstructed glacier beds justifies their application.

[3] The modeling approach GlabTop (Glacier bed Topography) as presented in *Paul and Linsbauer* [2012] and applied here is based on the assumption that glacier thickness depends on surface slope via an average basal shear stress (assuming perfect plasticity [cf. *Paterson*, 1994]), which depends on the mass turnover and, hence, the mass balance gradient and the elevation range of the considered glacier [*Haeberli and Hoelzle*, 1995], with an upper-bound value of 150 kPa for large glaciers (cf. also *Li et al.* [2012]). Using only three input data sets (glacier outlines, a DEM and a set of digitized central branch lines), GlabTop calculates thickness values at point locations and spatially interpolates them to a continuous bed within the limits of the glacier using the ANUDEM algorithm by *Hutchinson* [1989]. This algorithm is designed to create hydrologically correct DEMs and is thus especially suitable for glacier beds with their concave shapes [*Fischer*, 2009]. Based on the concept of simple map algebra (adding or subtracting grids) [e.g., *Etzelmüller and Björnsson*, 2000], GlabTop can be applied to large samples of glaciers in a computationally efficient manner.

[4] The regional scale application of the modeling framework presented in *Paul and Linsbauer* [2012] is presented in this study by applying GlabTop to all glaciers in Switzerland along with a detailed analysis and validation of the results. The main objectives of this study are thus: (a) the calculation of the ice thickness distribution for all glaciers in Switzerland, (b) the analysis of the geomorphometric characteristics of the modeled glacier beds with a focus on overdeepenings as sites of potential future lake formation, (c) a comparison of the here derived glacier volumes with results from other approaches, (d) a validation of model results with data from Ground Penetrating Radar (GPR), and (e) a determination of the sensitivity of GlabTop in regard to uncertainties of the input parameters used. For (d) we selected three differently shaped larger valley glaciers and for (c) we compared the modeled mean glacier thickness to the results from (i) a modeling approach based on principles of mass conservation and flow dynamics developed by *Farinotti et al.* [2009a] and (ii) the approach by *Haeberli and Hoelzle* [1995] using tabular data as stored in glacier inventories as an input.

[5] After describing the study region and input data sets, we summarize the previously and here-applied methods. We then present the results of the modeled ice thickness distribution together with the derived glacier volumes and potential lake formation sites. After presenting the model validation and comparison with other approaches, the results achieved and the accuracy and uncertainty of the model are discussed. The conclusions summarize the main findings.

2. Study Region

[6] The Swiss Alps cover an area of about 25000 km^2 (Figure 1) with glaciers in this region stretching from about 1500 up to 4500 m a.s.l. and a mean elevation of about 2900 m a.s.l. [*Paul et al.*, 2007a]. The 71 glaciers with an area larger than 3 km^2 (in 1973) contribute 58% to the total glacierized area but only about 3% to the total number. On the other hand, glaciers smaller than 1 km^2 account for 91% of the number but only 24% of the area (Figure 2a). However, these small glaciers contributed strongly to the overall area loss between 1985 and 1999 [*Paul et al.*, 2004] and are

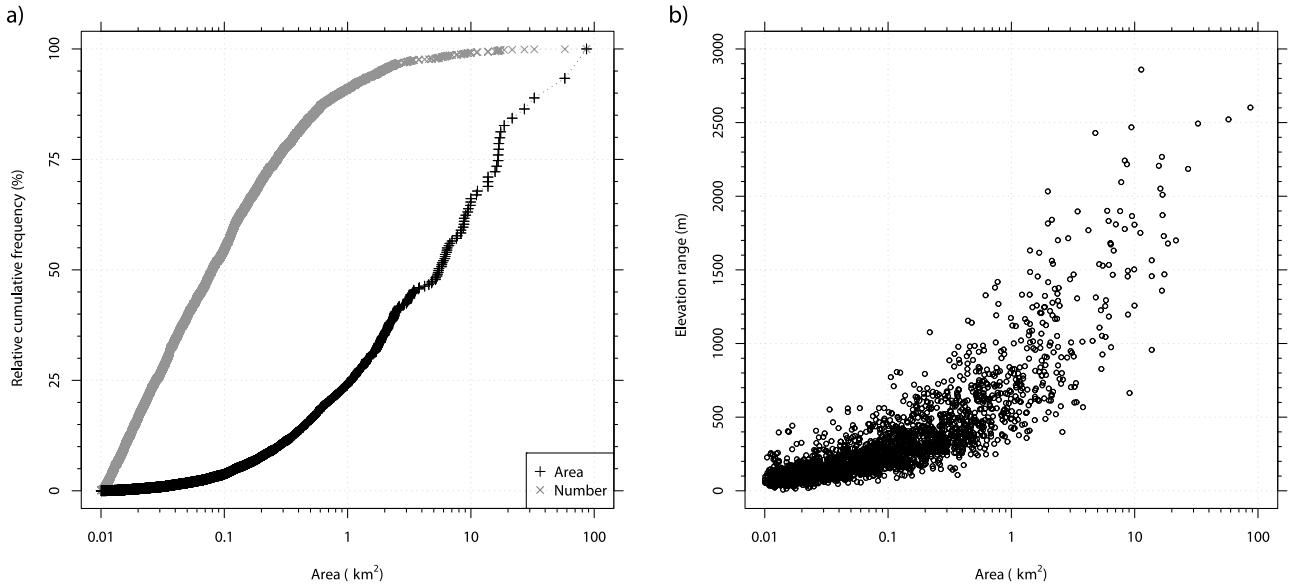

Figure 2. (a) Glacier size and the number of glacier versus the relative cumulative frequency of both values in the same plot. (b) Relation between glacier area and elevation range of all Swiss glaciers.

thus also considered in GlabTop. The strongly biased number and size distribution has to be considered when mean glacier thickness is interpreted.

[7] In total, we considered 2365 glaciers and glacierets larger than 0.01 km^2 (highlighted in Figure 1). Their elevation range is plotted against glacier area in Figure 2b. For glaciers with a size of about 10 km^2 the elevation range can vary between 700 and 2800 m and 38 glaciers stretch over more than 1600 m. From this sample of modeled glaciers, four sub-samples were selected for various purposes: (A) 71 glaciers larger than 3 km^2 for the comparison with thickness values modeled by *Farinotti et al.* [2009a], (B) five glaciers with large tongues reaching down to low altitudes for visualization of modeled glacier beds (in long profiles), (C) three glaciers (Rhone, Zinal and Corbassière) for validation of the model results with GPR soundings, and (D) one glacier (Morteratsch) for uncertainty tests. Morteratsch glacier (16 km^2) is composed of two main branches (Pers and Morteratsch glaciers) which merge in the lower third of the main valley. Rhone glacier (17 km^2) flows from its gently sloping accumulation basin to the comparably flat ablation area in an increasingly narrow valley, where the tongue ends today in a rapidly enlarging lake that fills an overdeepening behind a bedrock barrier. Zinal glacier (16 km^2) is composed of five major, comparably steep tributaries and has a flat, nearly completely debris-covered tongue. And finally Corbassière glacier (16 km^2) mainly consists of two flat basins in the accumulation area which are connected by moderately steep icefalls with a wide, flat and largely debris-free tongue as ablation area.

3. Data Sets

[8] GlabTop requires three different input data sets: (1) a DEM, (2) glacier outlines and (3) a set of branch lines for each glacier.

[9] The DEM used here was produced by the Swiss Federal Office of Topography (swisstopo) from aerial photography and has a cell size of 25 m. The DEM is based on the interpolation of contour lines from the Swiss topographic map sheets (1:25000) and includes digitized lake perimeters, main break lines and spot heights [*Rickenbacher*, 1998]. Two versions of this data set are available: a Level 1 (DHM25L1) from around 1985 and a Level 2 (DHM25L2) from around 1995. Apart from the acquisition date, the two DEMs primarily differ in regard to the algorithms used for the contour line interpolation [*Swiss Federal Office of Topography*, 2005]. For the Bernina region both DEMs refer to 1991. For the purpose of this study, we have evaluated the suitability of both DEMs.

[10] Digital glacier outlines from two sources were used: First, outlines based on the digitized Swiss Glacier Inventory from 1973 by *Müller et al.* [1976], in the revised version by *Maisch et al.* [2000]. These glacier polygons fit well to the glacier extent in the DHM25L1, as only small overall area changes took place for most glaciers in the Alps between 1973 and 1985 [*Paul et al.*, 2004]. Second, the glacier outlines from the Swiss Glacier Inventory 2000 (SGI2000) [*Paul*, 2007] as derived from Landsat images acquired in the years 1998 and 1999 are used. In this case the DHM25L2 corresponds much better to the extent of the glaciers. We only consider perennial ice bodies larger than 0.01 km^2 from these two samples containing 2365 glaciers and glacierets for 1973 and 1182 for 1998/1999. The difference in number is mainly due to the number of small glaciers considered (<0.1 km^2); many of them have disappeared during this time period or were not recognizable in the satellite image (e.g., due to increased debris cover) [*Paul et al.*, 2007a].

[11] The manually digitized central branch lines cover all important tributaries of a glacier and merge at confluences (they are thus not flow lines in a strict glaciological sense). The shaded relief of the DEM, elevation contour lines in 50 m equidistance, and if necessary, the Swiss topographic maps (1:25000) were used as background information to digitize them. According to the guidelines described in *Paul and Linsbauer* [2012], the branch lines were digitized from

bottom to top, perpendicular to the contour lines of surface elevation, ending about 100 m before the glacier outline with one parallel line for every 200–400 m of glacier width. The fully digitized branch line data set for the 1973 glacier extent was clipped and if necessary manually modified until the branch lines also matched the SGI2000 glacier outlines. Additionally, one central flowline, which directly connects the lowest with the highest point, was digitized for each glacier. In total, the digitizing of all vector lines (branch lines (4400 km) and central flowlines (2100 km) for the 1973 glacier extent, branch lines (3500 km) and central flowlines (1400 km) for the SGI2000) was performed in less than a week.

[12] GPR profiles for the three glaciers Rhone (7 profiles), Zinal (8 pr.) and Corbassière (11 pr.) were used for validation of the model results. They were provided by the Laboratory of Hydraulics, Hydrology and Glaciology (VAW), ETH-Zurich and for Corbassière digitized from the report by *Laboratory of Hydraulics, Hydrology and Glaciology* (*VAW*) [1998] and the work of *Farinotti* [2010]. The profiles from Rhone and Zinal have also been used in the study by *Farinotti et al.* [2009b] for model validation and the profiles of all three glaciers for estimating their glacier volume by *Farinotti et al.* [2009a]. They were acquired during different field campaigns (Rhone: 2003; Zinal 2006/2007; Corbassière: 1988/1998) [*Farinotti et al.*, 2009b, 2009a; *Farinotti*, 2010; *VAW*, 1998]. These profiles only provide glacier depth information at the respective cross sections and have uncertainties as well (2D-analysis, lateral effects not considered, smoothing effect of the sounding method). For the bed between these profiles a direct validation is not possible.

4. Previous Works on Glacier Thickness Modeling

[13] Thickness estimates for glaciers were long made using empirical relations between measured surface areas and (geophysically) measured ice depths [e.g., *Müller et al.*, 1976; *Maisch and Haeberli*, 1982; *Driedger and Kennard*, 1986; *Maisch et al.*, 2000] or volume/area correlations [e.g., *Chen and Ohmura*, 1990; *Bahr et al.*, 1997; *Luethi et al.*, 2008]. Neither area-related estimates nor other scalar approaches [e.g., *Haeberli and Hoelzle*, 1995] yield information about subglacial topography, a severe limitation which can now be overcome using digital terrain information and distributed thickness estimates [e.g., *Clarke et al.*, 2009].

[14] The topographic information which became available in detailed glacier inventories of the past century first made it possible to derive mean glacier thicknesses and hence volumes for large samples of glaciers using listed elevation ranges and lengths to derive mean slope values for each glacier [*Haeberli and Hoelzle*, 1995; *Hoelzle et al.*, 2007]. Corresponding thickness estimates for individual glaciers are considered to be more realistic than area-dependent estimates, because flow-related glacier thickness is strongly slope-dependent [*Paterson*, 1994; *Kamb and Echelmeyer*, 1986].

[15] The application of DEMs in combination with vector outlines of glacier extent now makes ice-depth estimates for individual parts of glaciers possible. Though such approaches have been presented long ago [*Driedger and Kennard*, 1986], they only recently became rather popular. Two examples of such recently developed methods with a focus on modeling glacier thickness distribution for large samples of glaciers were presented by *Clarke et al.* [2009] and *Farinotti et al.* [2009b].

[16] *Clarke et al.* [2009] used an Artificial Neural Network (ANN) to transfer the characteristics of now ice free glacier beds to contemporary glaciers. The ANN method yielded plausible subglacial topography with an error of ± 70 m, but is computationally very intensive and requires a repeated application in overlapping 50 km by 50 km subregions to cover a larger mountain range [*Clarke et al.*, 2009].

[17] The model ITEM (Ice Thickness Estimation Method) by *Farinotti et al.* [2009b] uses a method based on mass conservation and principles of ice flow dynamics to estimate the ice thickness distribution of larger alpine glaciers (>3 km^2). It requires a detailed parameterization of the involved physical processes and rough assumptions about several only vaguely determined processes (e.g., surface accumulation, mass balance gradient, rate factor in the ice flow law, basal sliding velocity). As a consequence, it must be tuned for each glacier [*Farinotti et al.*, 2009b] by comparing it with selected glacier cross sections derived from GPR profiles to make it realistic. The required model input data are glacier surface topography, glacier outlines delineating ice flow catchments and meteorological data to calculate mass balance distribution and estimate ice flow. The method also worked well for a larger number of glaciers, when the required amount of input (and calibration) data was available [*Farinotti et al.*, 2009a].

[18] *Li et al.* [2012] developed a method that is also based on the perfect-plastic rheology assumption (see equation (1)), for estimating the flow line thickness of glaciers. The novelty is the inclusion of side drag in the force-balance calculation; thus it requires accurate determination of the width of each cross-section from observations. The key advantage of this model is its simplicity: only few input data sets are required, they are straightforward to derive, and the physical basis is easy to understand. The uncertainty relates to the basal shear stress (τ), which has to be assumed where independent ice-thickness data are lacking, or to be calibrated in case such data is available.

[19] A critical step for the use of modeled glacier beds in other applications is the assessment of their quality, which requires validating them with ground truth data. For still existing glaciers, bedrock information can be derived from (hot-water) drilling, geophysical soundings like ground penetrating radar (GPR) or – optimally – a combination of both [*Haeberli and Fisch*, 1984]. Such reference information, however, is only sparsely available and in many cases biased toward crevasse-free, flat and thus thick glacier parts with compressing flow [e.g., *Frey et al.*, 2010]. The bed between the profiles remains unknown and a modeled product [e.g., *Fischer*, 2009; *Binder et al.*, 2009].

5. Methods

5.1. The GlabTop Approach

[20] The GlabTop approach introduced by *Linsbauer et al.* [2009] and *Paul and Linsbauer* [2012] is intermediate between the two approaches of *Clarke et al.* [2009] and

Farinotti et al. [2009b] and close to the idea by *Li et al.* [2012]: it is based on a very basic consideration of flow dynamics and it enables all glacier beds to be calculated at once which makes it computationally very fast. It is calibrated with geometric (shear stress) information from vanished (late glacial) glaciers and validated with independent GPR measurements.

[21] The technical details of GlabTop are described by *Paul and Linsbauer* [2012] and are thus only shortly summarized here. The core of GlabTop is the parameterization scheme presented by *Haeberli and Hoelzle* [1995] for analyzing tabular data in detailed glacier inventories. In that approach, a constant basal shear stress along the central flowline of the entire glacier is assumed to derive ice thickness along the central flowline:

$$h = \frac{\tau}{f \cdot \rho \cdot g \cdot \sin \alpha}, \tag{1}$$

with h = ice thickness, τ = basal shear stress, f = shape factor (0.8), ρ = ice density (900 kgm^{-3}), g = acceleration due to gravity (9.81 ms^{-2}) and α = glacier surface slope ($\alpha \neq 0$). For each glacier, a value for τ is estimated from an empirical relation between τ and elevation range (ΔH) according to a regression with a sample of values calculated for 62 vanished late glacial glaciers [*Maisch and Haeberli*, 1982; *Haeberli and Hoelzle*, 1995]:

$$\begin{aligned} &\tau = 0.005 + 1.598\Delta H - 0.435\Delta H^2, \\ &\textit{and } \tau = 150 \text{ kPa } \textit{for } \Delta H > 1600 \text{ m}. \end{aligned} \tag{2}$$

[22] A maximum value of 150 kPa is assumed for glaciers with $\Delta H > 1600$ m (38 in our sample) and the basal shear stress of the smallest glaciers is set to 0.005 kPa. The maximum value of 150 kPa is empirically estimated [*Maisch and Haeberli*, 1982; *Haeberli and Hoelzle*, 1995] and 50% higher than the 100 kPa used in other studies as a mean value for all glaciers. For example *Marshall et al.* [2011] mentioned that this value tend to underestimate the shear stress for large glaciers and overestimate it for small glaciers. This is in line with the study by *Driedger and Kennard* [1986] who found size-dependent values between 30 and 160 kPa for a group of comparably steep glaciers on the Cascade volcanoes and *Li et al.* [2012] who found values of 50–175 kPa for five Chinese glaciers.

[23] The variable parameters in the model are the basal shear stress (τ) and the surface slope (α). The shape factor (f), which is related to the lateral drag on a glacier through friction at the valley walls and the general form of the glacier cross section, ranges according to *Paterson* [1994] from 0.5 to 0.9. For alpine glaciers and based on empirical evidence *Maisch and Haeberli* [1982] used a shape factor of 0.7 for the glacier tongues in the ablation area and 0.9 for the much wider accumulation areas. *Haeberli and Hoelzle* [1995] chose $f = 0.8$ for the entire glacier in their parameterization scheme. To keep the processing in GlabTop simple, we also used a constant shape factor ($f = 0.8$) for all glaciers.

[24] Application of the perfect plasticity assumption of equation (1) including effects of longitudinal stress coupling requires that surface slope (α) is averaged over a reference distance, which is about one order of magnitude larger than the local ice thickness [*Paterson*, 1994; *Haeberli and Schweizer*, 1988; *Kamb and Echelmeyer*, 1986; *Maisch and Haeberli*, 1982]. Averaging surface slope within 50 m elevation bins results in reference distances of about 5–10 times the ice thickness.

[25] The basal shear stress (τ) is calculated from equation (2). The large spread of the data points found in *Haeberli and Hoelzle* [1995] reflects the general variability of flow dynamics (rate factor for ice deformation and relative amount of sliding) and cannot easily be overcome in any quantitative approach. The scatter relates to an uncertainty of ±30% and for some individual glaciers even ±45%.

5.2. GIS Implementation and Application to All Swiss Glaciers

[26] The spatial variability in ice thickness for an individual glacier is considered by calculating an averaged surface slope for equidistant elevation intervals of 50 m directly from the DEM. The reference distance for the slope determination is thereby automatically adjusted to the local glacier thickness, i.e., it is long where the glacier is relatively flat/thick and relatively short where it is steep/thin. Typical ratios of such reference distances versus local thickness vary here from 1:5 to 1:10.

[27] The subsequent spatial interpolation of the thickness values is performed with the ANUDEM (TopoToRaster in ArcGIS [*ESRI*, 2008]) interpolation scheme [*Hutchinson*, 1989] that was also used by *Fischer* [2009] for spatial interpolation of thickness profiles measured by GPR. The resulting digital map (raster data) of ice thickness distribution is subtracted from the surface DEM to obtain the bed topography, i.e., a DEM without glaciers. By calculating zonal statistics in the GIS, the key values for mean (h_{mean}) and maximum (h_{max}) ice thickness and total volume (V) are obtained. This mean thickness is also used for a comparison with the values derived by *Haeberli and Hoelzle* [1995] and from the ITEM approach [*Farinotti et al.*, 2009a].

[28] Both ice thickness distribution and bed topography were modeled for all ice bodies larger than 0.01 km^2, but a statistical analysis of the results is only performed for glaciers larger 0.1 km^2. Similar to *Haeberli and Hoelzle* [1995] we treat glacierets between 0.01 km^2 and 0.1 km^2 separately, using a mean ice thickness of 5 m and calculating the volume by multiplication with the ice-covered area. The overdeepenings in the glacier beds are detected by filling them with the ArcGIS hydrology-tool 'fill' [*ESRI*, 2008] and a slope grid derived from the filled DEM. By selecting slope values smaller than one degree within the glacier outlines, the overdeepenings in the glacier beds are found. The difference grid between the filled DEM and the former DEM without glaciers is used to quantify the area and volume of the overdeepenings. The mean and maximum depths of the potential lakes are also calculated with zonal statistics.

[29] In the implementation of GlabTop as presented by *Paul and Linsbauer* [2012], a standard Inverse Distance Weighted (IDW) interpolation was applied to have continuous thickness values between the base points, where the ice thickness is estimated according to the physical background (see section 5.1). Changing this 'IDW'-interpolation in GlabTop to the 'TopoToRaster'-algorithm entails a stronger smoothing of the subglacial topography with less artefacts and somewhat larger mean thickness values. To also consider the uncertainty related to the interpolation methods, we show selectively results from both modeling approaches.

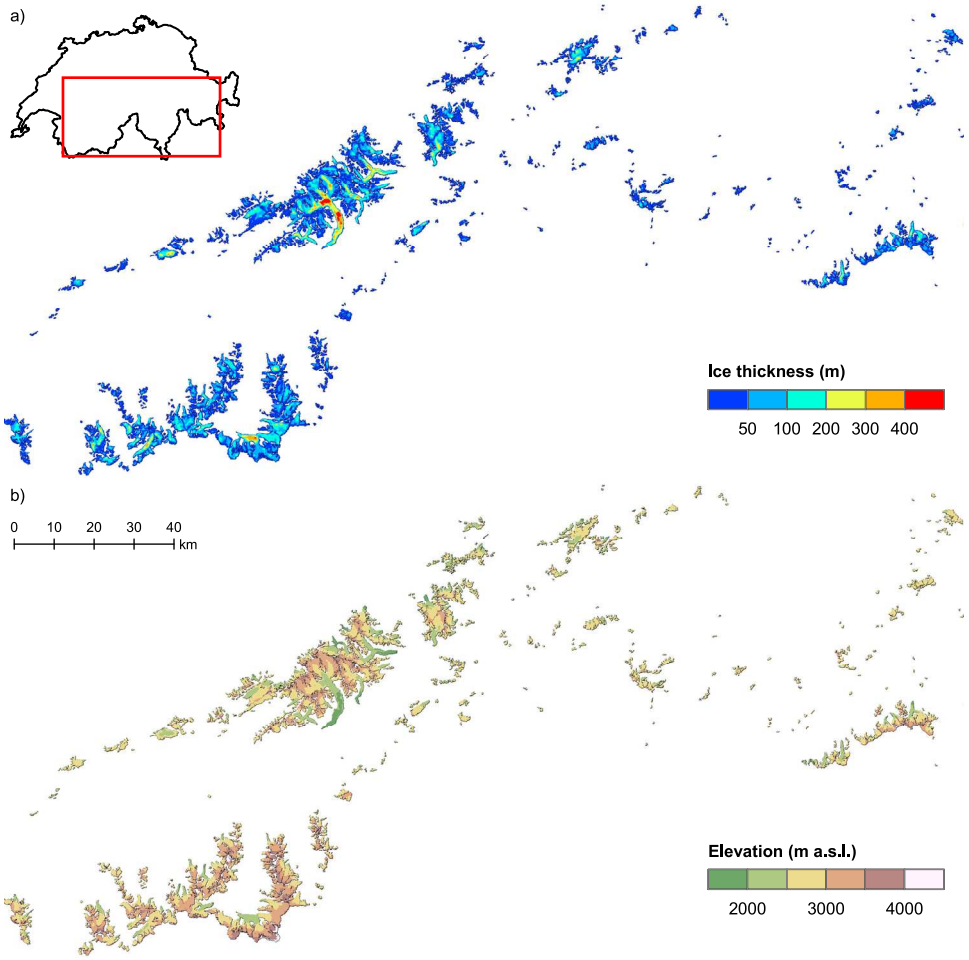

Figure 3. Output of GlabTop model run 73L1 (with the DHM25L1, the outlines from 1973 and the corresponding branch lines): (a) ice thickness distribution and (b) glacier bed elevation for all Swiss glaciers.

5.3. Accuracy Assessment, Uncertainty and Comparison of Methods

[30] For a validation of the model calculations, the results of GlabTop are compared to GPR cross sections (z values at given x, y coordinates) from three valley glaciers (Rhone, Zinal and Corbassière). The GPR profiles are typically located on accessible, flat and uncrevassed parts of the glacier surface (see Figure 8 and *Fischer* [2009]), i.e., where the glacier ice is thickest. To illustrate the differences resulting from the two applied interpolation methods in GlabTop (IDW and TopoToRaster), we show results from both methods in the cross-section comparisons.

[31] As also the input parameters shear stress, surface slope and shape factor have an uncertainty, we tested the impact of this uncertainty on the modeled ice thickness by a systematic variation of their values within typical uncertainty ranges (τ: $\pm$30%, α: $\pm$10%, f: $\pm$12.5%). The uncertainty for f assumes that typical values range from 0.7 to 0.9 instead of the here used value of 0.8 (see section 5.1). The assumed uncertainty in the slope value mainly results from local artefacts in the DEM, as elevation values (and hence also slope) of neighboring cells are otherwise highly correlated. This experiment revealed that the uncertainty in the modeled ice thickness is dominated by the uncertainty of τ. We have thus also modeled all glacier beds with 30% higher and lower values of τ and include the resulting thickness values in the comparison with the GPR profiles.

[32] For the comparison with the results from the ITEM approach we computed mean glacier thickness from the areas and volumes listed in *Farinotti et al.* [2009a]. As their values refer to the 1999 period, we used glacier outlines from the SGI2000 and the DHM25L2 as an input to GlabTop. As glacier outlines and input DEMs differ, also thickness values will likely not be the same. However, mean thickness is at least much less sensitive to differences in the glacier size than volume.

[33] We also compared our modeled thickness values with the approach by *Haeberli and Hoelzle* [1995], who used a set of widely available glacier inventory data (glacier length (L_0), maximum and minimum elevation (H_{max}, H_{min}) and surface area (A) to estimate glacier mean thickness. For this purpose we used the DEM, glacier outlines and central flowlines to derive the above parameters. Though both approaches are based on the same equations for calculation of mean ice thickness and τ, we consider them as independent enough for a comparison as the input data sets used are

Table 1. Glacierized Area (A) and Ice Volume (V) of Five Ice Thickness Classes as Modeled for the Year 1973 With GlabTop and the Two Different Interpolation-Methods for the Basepoints

Ice Thickness (m)	IDW(73L1)				TopoToRaster(73L1)			
	A (km^2)	%	V (km^3)	%	A (km^2)	%	V (km^3)	%
0–50	821	63	15	21	795	61	15	20
50–100	274	21	19	27	274	21	19	24
100–200	156	12	22	30	170	13	24	30
>200	52	4	16	22	65	5	21	26
Total	1304	100	72	100	1304	100	79	100

calculated differently and are statistically independent. Moreover, we are interested in the effects of a change in the source data (locally derived mean surface slope versus slope calculated from length and elevation range of a glacier) when equations are the same. Of course, this is a model intercomparison rather than validation.

6. Results

6.1. Ice Thickness Distribution and Total Volume of the Swiss Glaciers

[34] GlabTop was applied to the DHM25L1 with the glacier outlines from 1973 (GlabTop_73L1) and to the DHM25L2 with the outlines from the SGI2000 (GlabTop_2kL2) and corresponding branch lines for both combinations. We focus in the following on the results obtained with 'GlabTop_73L1' with the TopoToRaster-interpolation. In Figure 3 the ice thickness distribution (Figure 3a) and elevation of the resulting glacier beds (Figure 3b) for all Swiss glaciers is visualized.

[35] The ice thickness distribution reveals that ice thicknesses of less than 100 m (blue colors) are clearly dominant. Over approximately 60% of the glacierized area the ice is less than 50 m and over another 20% between 50 and 100 m thick. The large area of ice (about 800 km^2) which is only up to 50 m thick, contributes about the same amount or even less to the total volume of all glaciers than the small area (60–70 km^2) with ice thicknesses exceeding 200 m (cf. Table 1). Overall, the 3, 6 and 15 largest glaciers contain 1/4, 1/3 and 1/2 of the total ice volume respectively (cf. also Table 5).

[36] For the year 1973, we have estimated the total ice volume of all Swiss glaciers to be around 79 $\pm$ 23 km^3. Dividing the total ice volume by the total area of 1304 km^2 yields a corresponding (area weighted) mean ice thickness of 61 m (cf. Table 2). When excluding the largest 3, 6 or 15 glaciers, the mean thickness of all other glaciers is 50 m, 47 m and 40 m respectively. The mean thickness value is thus strongly influenced by the (few) largest glaciers. The comparison of modeled mean and maximum ice thickness per glacier (Figure 4a) reveals a high correlation of $R^2 = 0.95$ (linear regression with a slope of $y = 2.99x$ and an intercept of 0). This implies that maximum ice thickness is generally about three times larger than mean ice thickness, which is in good agreement with the value of 2.9 found by *Raper and Braithwaite* [2009] from theoretical considerations.

[37] When glacier area is plotted against modeled mean glacier thickness for each glacier in the analysis (Figure 4b), the wide range of possible mean thickness values for glaciers of the same size becomes obvious, although the double logarithmic plot strongly reduces the scattering. It also seems that a simple power law does not accurately fit the data points.

[38] An ice volume of 68 $\pm$ 20 km^3 and a mean ice thickness of 65 m is obtained by the model run 'GlabTop_2kL2' for the year 2000 (cf. Table 2). This gives a total volume loss of 11 km^3 between 1973 and 2000, which is in good agreement with the 12.2 km^3 volume loss derived from direct DEM differencing and comparison with surface mass balance measurements [*Paul and Haeberli*, 2008]. Assuming little volume change between 1973 and 1985 [*Paul et al.*, 2004] this gives a volume loss of about -17% for the Swiss glaciers in 15 years or a loss rate of about 1% per year. Further results for individual glaciers and distinct area classes can be found in Table 5.

6.2. Glacier Bed Topography

[39] The modeled glacier bed elevations are shown in Figure 3b. In regions with large ice thickness, the elevations of the glacier beds are comparably low. This can also be seen in the direct comparison of bed elevation profiles along the central flowline of five large glacier tongues in Figure 5. Large parts of these tongues are located on bedrock with elevations below 2400 m a.s.l.. Great Aletsch and Unteraar glacier have major parts of their beds even below 2000 m a.s.l. (Figure 5). The profile lines also illustrate the large number of modeled overdeepenings (cf. section 6.3). This "step-pool" character of glacier beds is found in several deglaciated mountain ranges and will likely facilitate the formation of dead ice during glacier retreat and hence its rapid melt down [*Vacco et al.*, 2010], as well as possible lake formation in the future [*Frey et al.*, 2010]. Further

Table 2. Total Glacierized Area (A), Mean Ice Thickness (h_{mean}) and Total Volume (V) of 3 GlabTop Model Runs With Different Input Data for the IDW and the TopoToRaster-Interpolation

				IDW		TopoToRaster	
Run	Outlines	DEM	A (km^2)	h_{mean} (m)	V (km^3)	h_{mean} (m)	V (km^3)
73L1	1973	DHM25L1	1304	55	72	61	79
2kL1	SGI2000	DHM25L1	1040	61	64	67	70
2kL2	SGI2000	DHM25L2	1035	59	61	65	68

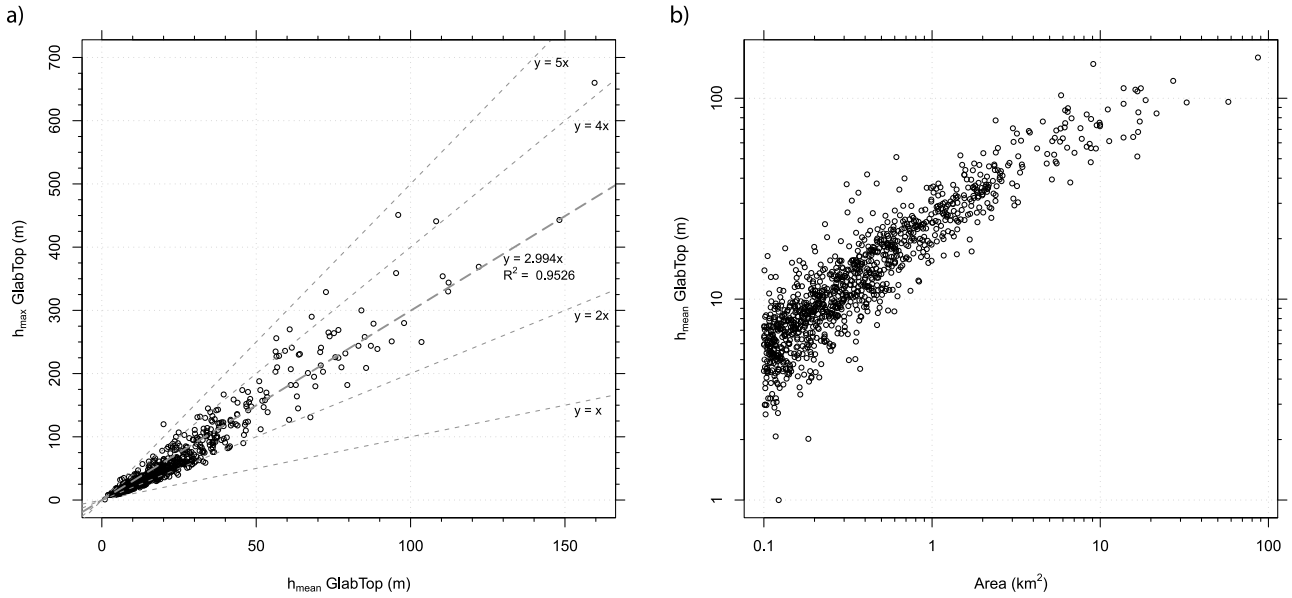

Figure 4. (a) Scatterplot of mean thickness versus maximum thickness and (b) mean thickness versus area.

profiles through other glaciers (not shown) illustrate the variability of the location of the thickest glacier parts. While for most of the larger valley glaciers the thickest ice is found in the flat tongues of the ablation region, for some glaciers (e.g., Trient, Giétro, Mont Miné, Ried, and Hüfi glacier) it is found in the accumulation region. These glaciers have comparably steep and thus thin tongues and a wide and flat (and thus thick) accumulation area at high altitude. This has important consequences for the future evolution of glaciers in regard to water resources (cf. section 8.3).

[40] The mean ice thickness for distinct elevation intervals with reference to the modeled glacier bed is depicted in Figure 6, along with the hypsography of the glacier surface and the volume distribution of the ice (both for 1973). While the glacierized area is about normally distributed around the mean elevation of 2900 m a.s.l., the mean ice thickness reaches its largest values at much lower elevations, i.e., 1900 m a.s.l..To some extent, this peak can be related to the large overdeepening found at Konkordia (the confluence of three large branches) of Great Aletsch glacier (cf. section 6.3). But also in general, much higher ice thickness values are found over bedrock situated below 2500 m a.s.l. The volume distribution resulting from the distribution of areas and thickness with elevation follows the hypsometry of the surface area with a downward shift of about 200 m. Despite the rapid decrease of glacier area below 2500 m a.s.l. (with reference to the surface), the ice volume situated above such low altitudes remains important (Figures 3 and 6).

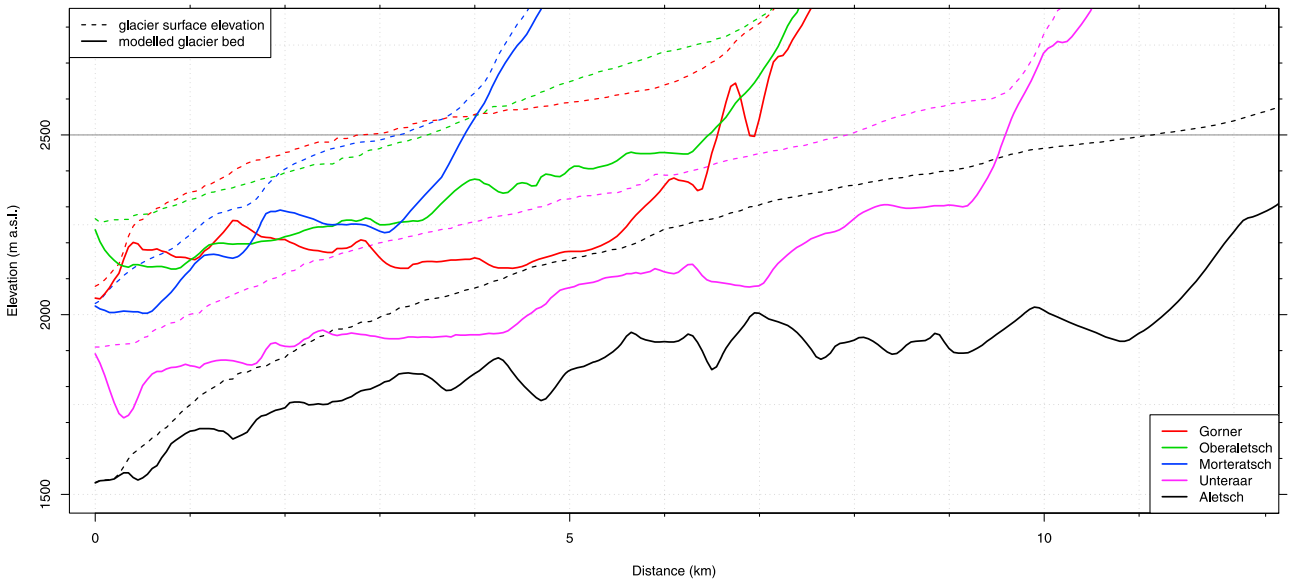

Figure 5. A direct comparison of profiles of bed elevations along the central flowline for a subset of 5 larger glacier tongues. For location see Figure 1.

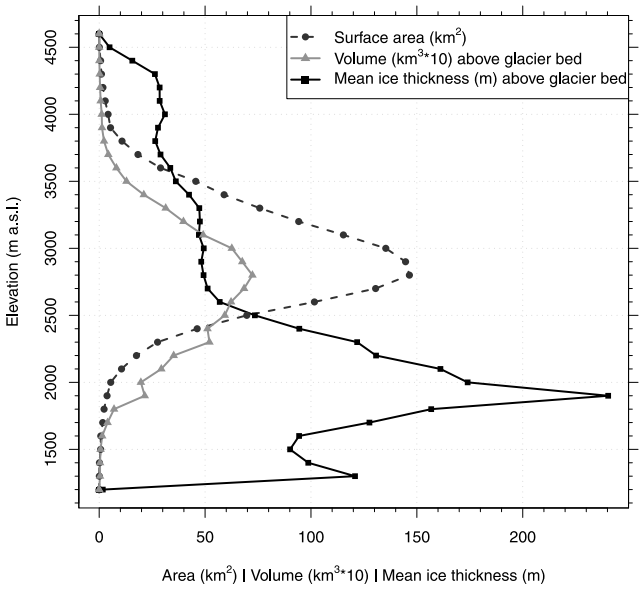

Figure 6. The hypsographic distribution of the glacier area and volume for the year 1973 and the corresponding mean ice thickness for distinct elevation intervals related to the modeled glacier bed.

6.3. Overdeepenings and Potential Future Lakes

[41] The detected overdeepenings in the modeled glacier beds indicate a high number of sites enabling potential future lake formation [cf. *Frey et al.*, 2010]. Using a threshold of 1 ha (10000 m^2) for the lake area (to exclude insignificant water bodies and model artifacts), 500–600 sites remain for the GlabTop_73L1 model run and 400–500 for the GlabTop_2kL2 run. For the Aletsch region a map with outlines of the modeled overdeepenings from both model runs is shown in (Figure 7a). The congruence of many outlines indicates that the location of these features is rather robust i.e., not much influenced by the DEM selected. These local depressions may, depending on the rocky/sedimentary nature of the glacier bed [e.g., *Maisch et al.*, 2000; *Zemp et al.*, 2005], be either filled with water and form lakes (deep depressions, rock beds) or trap sediments and become floodplains (shallow depressions, sediment beds) in the glacier forefield after the glacier has disappeared. Disregarding the latter case for a first order assessment, a total of about 50–60 km^2 of potential new lake area can form (Table 3) once all glacier ice has vanished [cf. *Künzler et al.*, 2010]. This is slightly more than the area of Lake Thun (48.4 km^2) in Switzerland (Bundesamt für Umwelt (BAFU), Seen in der Schweiz, unpublished data, 2007, http://www.bafu.admin.ch/hydrologie/01835/02118/index.html).

Table 3. Summary of the Overdeepenings Detected in the Modeled Glacier Bed Geometries for Two GlabTop Runs and Two Interpolation-Algorithms[a]

	IDW		TopoToRaster	
	73L1	2kL2	73L1	2kL2
Number of overdeepening	625	523	515	394
Total area (km^2)	65	52	56	44
Total volume (km^3)	2.3	1.6	1.9	1.2
Arithmetic mean depth (m)	35	31	35	28
Area weighted mean depth (m)	15	15	14	13

[a](IDW, TopoToRaster): 73L1 refers to the year 1973 and 2kL2 refers to the year 1999.

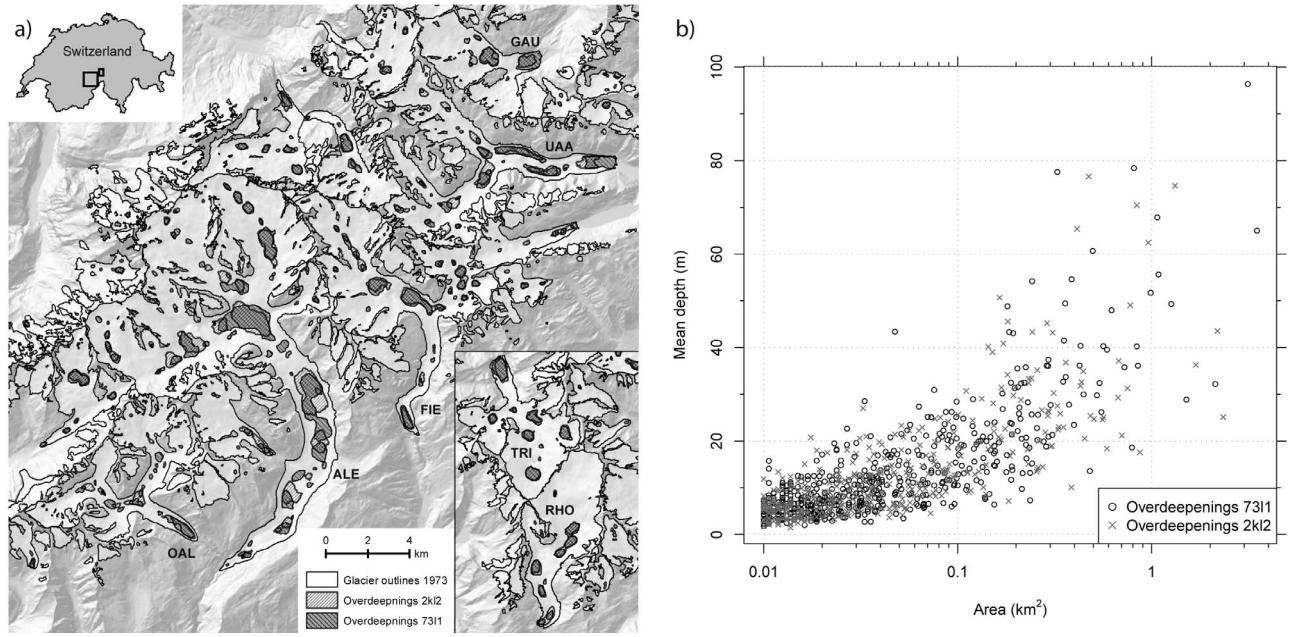

Figure 7. (a) An illustration of the modeled overdeepnings for both model runs for the Aletsch region (see inset for location; abbreviations refer to the following glaciers: GAU, Gauli; UAA, Unteraar; FIE, Fiescher; ALE, Great Aletsch; OAL, Oberaletsch; TRI, Trift; RHO, Rhone) and (b) scatterplot of mean depth of the overdeepenings versus their area as modeled for the year 1973 (73L1) and 1999 (2kL2).

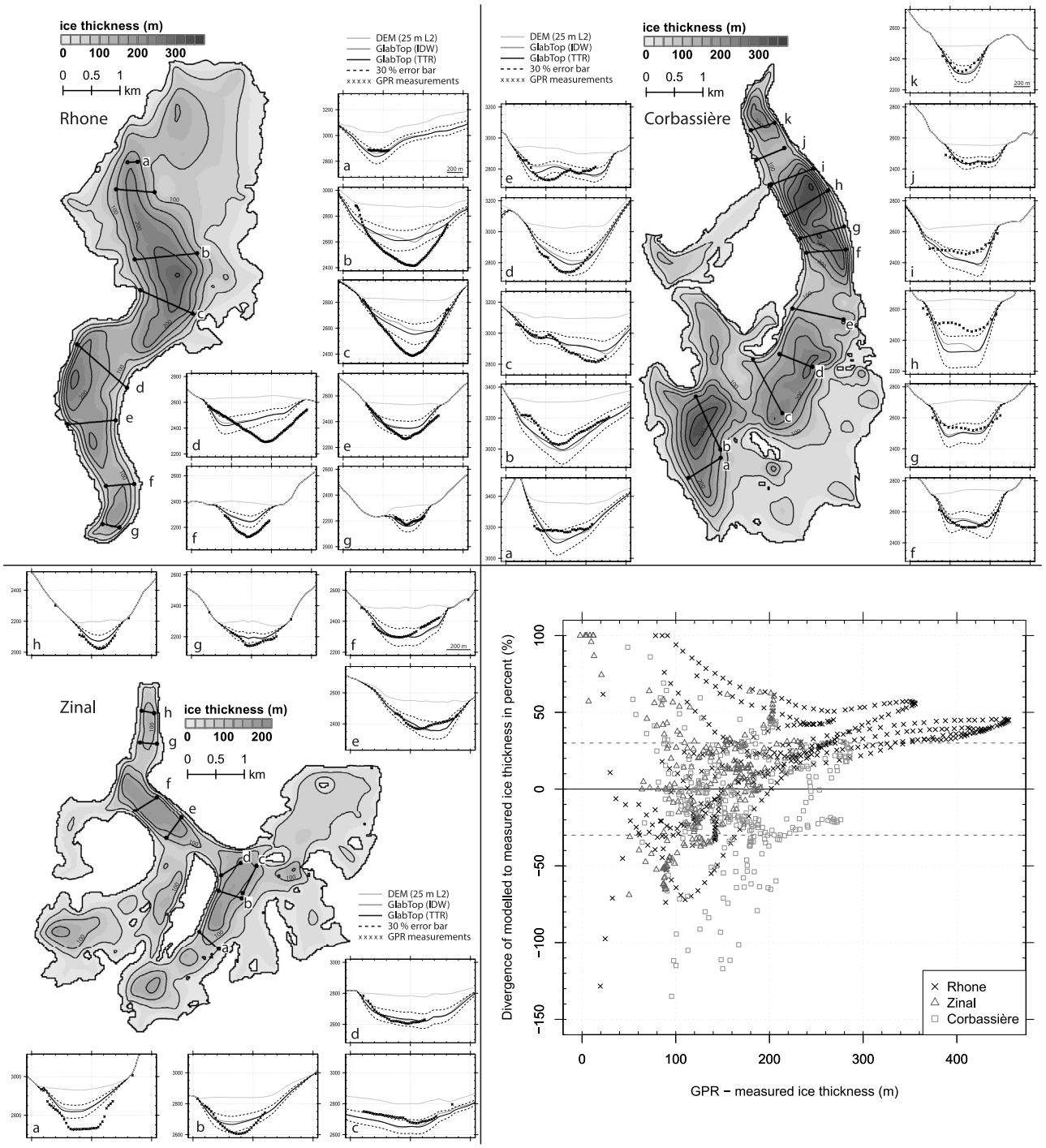

Figure 8. (top left) Calculated ice-thickness distribution of Rohne, (top right) Corbassière and (bottom left) Zinal glacier. The insets show the marked cross-sections with the two different GlabTop model versions (IDW versus TopoToRaster), the GPR measurements and an error range of ±30% for validation. All profile plots have the same horizontal extent and vertical exaggeration. On the y-axis the elevation is displayed. (bottom right) Divergence of modeled to measured ice thickness value in percent of the three validation glaciers is assigned to the measured thickness value from GPR.

[42] More than half of the 500–600 overdeepenings are smaller than 5 ha and their mean depth is smaller than 20 m (Figure 7b). The two largest overdeepenings are located underneath Great Aletsch glacier with a combined area of about 5 km^2. The depression located at Konkordia, for instance, has an area of about 2.5 km^2, a mean (max) depth of approximately 100 m (300 m) and a volume of about 250 million m^3 (Figure 7a). This roughly corresponds to the Lac d'Emosson, which is the second largest hydropower lake in the Swiss Alps (BAFU, unpublished data, 2007) with an

Table 4. Mean Thickness in Meters of the Three Validation Glaciers (Rhone, Zinal and Corbassière) Derived With the Approach From *Haeberli and Hoelzle* [1995] and GlabTop (Two Interpolation Methods) From the DEM25L2 and the SGI2000 Outline and Also for the ITEM Approach Where the Calculated Volume was Divided With the Area as Listed in *Farinotti et al.* [2009a]

	HH95	GT(idw)	GT(ttr)	ITEM
Rhone	105	101	105	132
Zinal	54	58	61	66
Corbassière	84	91	96	93

area 3.27 km^2 and a volume of 227 million m^3, respectively. The largest mean depth of the potential lakes would reach 100 m, but most of them have a mean depth of less than 50 m (Figure 7b). Two-thirds of the overdeepenings have a volume below 1 million m^3 and about 50 have a volume larger than 10 million m^3. The total volume of all modeled overdeepenings is about 2 km^3 or about 3% of the estimated ice volume in the Swiss Alps today.

7. Evaluation of Model Performance

7.1. Comparison With GPR Profiles

[43] In Figure 8 the calculated ice thickness distributions of the validation sites (Rhone, Corbassière and Zinal glacier) are shown within the SGI2000 outlines and the location of the GPR-measurements. The cross-section plots show elevation versus distance as modeled by GlabTop with two interpolation methods, a ±30% uncertainty range for the TopoToRaster-interpolation and the GPR measurements. This comparison reveals that GlabTop generally models the parabolic shape of glacier beds in good agreement with the shape of the GPR measurements. In absolute terms, the GPR data often show lower elevations (or higher ice thickness, in particular for Rhone glacier), but they are nearly always within the ±30% uncertainty range. Comparing the measured and modeled mean and maximum ice thickness within a profile at the locations of the GPR measurements, only 6 (mean) or 10 (maximum) out of 26 profiles deviate more than 30% and only 1 (mean and max) by more than 50%. For Zinal and Corbassière glacier the differences are not systematic and GlabTop is sometimes closer to the GPR data than ITEM. Only few profiles differ obviously from the measurements and need further explanation. Mean thickness values for the entire glacier are compared in Table 4. For Rhone glacier the value derived by GlabTop is about 20% smaller than with ITEM, for the other two glaciers there is not a large difference.

[44] At *Zinal glacier* (Figure 8, bottom left) ice thickness with GlabTop and ITEM is underestimated at profiles (a) by about 90 m and (b) by about 60 m. Compared to the ice thickness distribution modeled by ITEM [*Farinotti et al.* 2009b, Figure 7], GlabTop produces very similar results at the visual scale, in depth as well as in the location of the deeper and shallower parts. For 9 out of 11 profiles at *Corbassière glacier* (see Figure 8, top right) the measured GPR values are within the 30% uncertainty range of the modeled ice thickness with GlabTop. Only at profile (h) GlabTop strongly overestimates ice thickness (by about 150 m). This is different for *Rhone glacier* (see Figure 8, top left), where both methods often underestimate the GPR-derived thickness value, in particular the thickest parts (by more than 100 m). To obtain a better fit at these places (profiles b and c), a 50% higher ice thickness and hence a shear stress of about 225 kPa would be required for GlabTop. This seems unrealistically high for such flat regions and hints to specific local processes that are not accounted for by either model. Also special is profile (d), where GlabTop modeled an overdeepening at the orographic right side of the glacier tongue (where the surface is very flat) that does not appear in the GPR data. This illustrates that local surface slope might not in all cases be a good predictor of glacier thickness. However, based on visual inspection there is a good general agreement of the modeled thickness distribution pattern between GlabTop (Figure 8, top left) and ITEM [*Farinotti et al.* 2009b, Figure 6].

[45] The point-to-point comparison between modeled and measured ice thickness as shown in Figure 8 (bottom right) can be used for an integrative uncertainty assessment. In total, 54% of the differences are smaller than ±30% while 82% are smaller than ±50%. In particular for the large ice thicknesses at Rhone glacier the modeled values are out of the range of ±30%. For Zinal and Corbassière glacier 58% and 67% of the modeled values are within the ±30% uncertainty range. Some values differ by more than ±100%, but this concerns a small number of points with mostly thin ice. The overall mean difference is 6% with a standard deviation of 46%. Given that both models (GlabTop and ITEM) are not really designed to reproduce glacier thickness value at a point scale (i.e., the GPR profiles) we consider the agreement as sufficient for the intended purposes. The general pattern of the ice thickness distribution as well as the location of overdeepenings in the bed rock are rather robust and thus appropriate for application in other models.

7.2. Uncertainties in Input Parameters

[46] The uncertainty of each factor (cf. equation (1)) propagates in the same way to the overall uncertainty of the modeled ice thickness as the latter results from a linear combination of all factors. This implies that the parameter with the highest uncertainty (τ) governs the uncertainty of the thickness estimates. With our assumed uncertainty ranges for the other parameters, we can also calculate a worst-case scenario where possible uncertainties act in the same direction. Under such conditions τ would be 30% lower (or higher), slope would be overestimated (or underestimated) by 10%, and f is 0.9 (0.7) rather than 0.8. In these cases the thickness values would be underestimated by 42% or overestimated by 62% compared to a reference value. This range might indicate a possible minimum and maximum deviation for individual glaciers. For most of the other combinations the difference to the reference value does not exceed ±30%.

7.3. Model Intercomparison

[47] Glacier thickness values derived from the approach by *Haeberli and Hoelzle* [1995] are listed in Table 5 for 71 glaciers larger than 3 km^2 and are compared in the scatterplot of Figure 9a with the values derived from GlabTop with the TopoToRaster-interpolation. The mean ice thickness of

Table 5. The Parameters Area (A_{73}), Elevation Range (ΔH) and Mean Slope (α) for 71 Glaciers >3 km^2 and a Comparison of Mean (h_{mean}) and Maximum Thickness (h_{max}) and Volume (V) as Modeled With GlabTop_73L1 With the IDW-Interpolation ($GlabTop_{idw}$) and the TopoToRaster-Interpolation ($GlabTop_{ttr}$) and the Parameterization Scheme From *Haeberli and Hoelzle* [1995] (HH95)[a]

	Glacier Parameter			h_{mean} (m)			h_{max} (m)			Volume (km^3)		
					GlabTop			GlabTop			GlabTop	
	A_{73} (km^2)	ΔH (m)	α (°)	HH95	idw	ttr	HH95	idw	ttr	HH95	idw	ttr
Grosser Aletsch Gletscher	86.63	2602	15.3	148	144	160	606	669	660	12.86	12.51	13.82
Gornergletscher	57.77	2522	18.9	91	87	96	442	416	451	5.26	5.00	5.55
Fieschergletscher VS	32.65	2493	18.2	104	87	95	429	365	359	3.39	2.83	3.11
Unteraargletscher	27.15	2186	17.9	103	112	122	683	369	369	2.80	3.04	3.31
Oberaletschgletscher	21.62	1700	21.5	91	78	84	465	298	300	1.96	1.68	1.82
Findelengletscher	18.62	1679	14.9	85	89	98	428	290	280	1.59	1.66	1.82
Rhonegletscher	17.44	1470	14.8	103	99	112	451	339	330	1.80	1.72	1.96
Triftgletscher	17.18	1729	19.5	71	69	77	252	282	269	1.21	1.19	1.32
Zmuttgletscher	16.85	1872	19.1	74	78	85	435	274	258	1.24	1.31	1.43
Morteratsch Vadret da	16.79	2010	21.6	64	66	68	296	304	290	1.08	1.11	1.15
Otemma Glacier d'	16.64	1359	16.9	110	96	108	601	398	441	1.83	1.60	1.80
Feegletscher	16.62	2267	23.4	42	51	51	184	178	174	0.70	0.84	0.85
Corbassière Glacier de	16.18	2052	16.8	84	97	110	431	392	354	1.36	1.57	1.79
Zinal Glacier de	15.70	2206	23.3	59	56	64	281	219	231	0.93	0.87	1.01
Hüfifirn	13.77	1565	14.7	70	99	112	241	356	344	0.97	1.37	1.55
Kanderfirn	13.76	956	14.1	88	80	94	379	252	251	1.22	1.11	1.29
Gauligletscher	13.76	1458	20.2	72	59	64	346	231	230	0.99	0.82	0.88
Fieschergletscher BE	11.31	2860	24.0	51	57	61	237	212	207	0.58	0.65	0.69
Mont Miné Glacier du	11.09	1751	16.9	80	79	88	290	279	279	0.89	0.87	0.98
Allalingletscher	9.98	1807	17.8	63	62	74	275	253	259	0.62	0.62	0.74
Brenay Glacier du	9.96	1257	19.7	71	59	73	346	253	329	0.71	0.59	0.72
Ferpècle Glacier de	9.90	1503	17.1	69	65	76	254	217	226	0.69	0.64	0.75
Langgletscher	9.52	1866	20.2	64	67	73	302	272	265	0.61	0.63	0.70
Oberer Grindelwaldgletscher	9.42	2468	24.5	48	54	56	169	203	203	0.45	0.51	0.53
Plaine Morte Glacier de la	9.09	664	7.70	76	124	148	272	402	443	0.69	1.12	1.35
Forno Vadrec del	8.82	1197	19.0	82	76	79	403	238	232	0.72	0.67	0.70
Steingletscher	8.81	1494	21.8	57	52	57	247	269	256	0.50	0.46	0.50
Roseg Vadret da	8.78	1455	21.9	57	49	48	234	167	160	0.50	0.43	0.42
Obers Ischmeer	8.65	2217	24.8	54	54	59	227	237	236	0.47	0.47	0.51
Mittelaletschgletscher	8.31	1778	24.0	53	54	57	284	216	228	0.44	0.45	0.48
Riedgletscher	8.31	2242	19.5	50	80	83	203	248	244	0.42	0.66	0.69
Saleina Glacier de	7.77	2096	22.2	54	60	63	221	188	182	0.42	0.46	0.49
Mont Durand Glacier du	7.63	1900	20.4	54	67	71	293	240	241	0.41	0.51	0.54
Tschierva Vadret da	7.03	1809	25.4	53	49	54	254	163	163	0.37	0.34	0.38
Brunegggletscher	6.75	1631	18.3	51	72	80	267	182	182	0.34	0.48	0.54
Palü Vadret da	6.64	1466	22.8	47	38	38	206	130	122	0.31	0.25	0.25
Griesgletscher	6.43	975	13.5	76	79	89	371	250	239	0.49	0.51	0.57
Trient Glacier du	6.40	1672	17.4	52	76	86	171	222	209	0.33	0.48	0.55
Moming Glacier de	6.36	1682	25.3	42	53	57	219	199	210	0.27	0.34	0.36
Tschingelfirn	6.19	1184	17.1	46	67	75	291	283	264	0.29	0.41	0.47
Arolla Glacier d'	6.18	1534	17.1	56	76	87	232	257	244	0.35	0.47	0.54
Rosenlauigletscher	6.14	1832	20.1	49	66	72	202	203	203	0.30	0.40	0.44
Turtmanngletscher	5.99	1901	19.3	58	59	63	252	168	164	0.35	0.35	0.38
Giétro Glacier du	5.85	1295	13.5	55	99	104	242	251	250	0.32	0.58	0.61
Arolla Haut Glacier d'	5.81	1045	18.5	57	69	71	338	231	234	0.33	0.40	0.41
Moiry Glacier de	5.77	1254	18.8	60	53	61	242	217	270	0.35	0.31	0.35
Hohlichtgletscher	5.51	1529	23.2	49	46	47	213	146	142	0.27	0.25	0.26
Schwarzberggletscher	5.48	925	14.9	58	67	69	311	183	180	0.32	0.37	0.38
Furgg-Gletscher	5.43	1053	20.6	54	47	48	283	142	148	0.25	0.22	0.22
Mellichgletscher	5.37	827	16.2	50	60	64	320	137	145	0.27	0.32	0.34
Oberaargletscher	5.32	1226	19.8	36	48	52	181	150	147	0.19	0.26	0.28
Dammagletscher	5.18	1107	20.3	63	60	61	302	181	182	0.33	0.31	0.32
Üsser Baltschiedergletscher	5.16	1539	26.1	37	38	39	165	114	117	0.19	0.20	0.20
Bisgletscher	4.84	1312	22.5	35	49	53	181	157	158	0.17	0.24	0.26
Paradiesgletscher	4.81	2429	28.0	32	43	47	131	177	171	0.15	0.20	0.23
Cheilon Glacier de	4.56	1017	16.9	50	66	77	322	215	225	0.23	0.30	0.35
Stufesteigletscher	4.21	1770	27.1	35	53	56	180	240	235	0.15	0.22	0.24
Tsanfleuron Glacier de	3.81	569	10.0	55	64	68	243	134	131	0.21	0.25	0.26
Castel Nord Vadrec dal	3.76	1013	18.9	57	61	69	415	186	195	0.22	0.23	0.26
Hohberggletscher	3.45	1897	25.1	41	45	45	180	192	174	0.14	0.15	0.16
Breithorngletscher	3.42	1307	23.5	41	45	47	219	152	148	0.14	0.15	0.16
Oberer Theodulgletscher	3.38	602	12.7	38	47	62	223	110	241	0.13	0.16	0.21
Wildstrubelgletscher	3.34	731	18.2	39	37	43	169	121	159	0.13	0.12	0.14
Silvrettagletscher	3.25	707	13.7	53	48	51	252	112	112	0.17	0.16	0.17
Grialetsch Vadret da	3.24	599	19.5	24	30	30	88	65	61	0.08	0.10	0.10

Table 5. (continued)

	Glacier Parameter			h_{mean} (m)			h_{max} (m)			Volume (km^3)		
					GlabTop			GlabTop			GlabTop	
	A_{73} (km^2)	ΔH (m)	α (°)	HH95	idw	ttr	HH95	idw	ttr	HH95	idw	ttr
Tiefengletscher	3.20	912	22.2	39	37	37	181	138	128	0.13	0.12	0.12
Tsijiore Nouve Glacier de	3.20	1469	21.6	54	56	67	222	194	201	0.17	0.18	0.21
Flachensteinfirn	3.09	937	25.4	30	29	29	125	59	57	0.09	0.09	0.09
Glatt Firn	3.05	1007	17.3	40	58	61	137	134	127	0.12	0.18	0.19
Alpjergletscher	3.04	703	19.1	32	31	32	123	81	78	0.10	0.09	0.10
Brunnifrin	3.02	949	18.1	44	57	71	211	220	213	0.13	0.17	0.21
	Glacier Parameter			h_{mean} (m)			h_{max} (m)			Volume (km^2)		
					GlabTop			GlabTop			GlabTop	
	A_{73} (km^2) sum	ΔH (m) mean	α (°) mean	HH95 mean	idw mean	ttr mean	HH95 mean	idw mean	ttr mean	HH95 sum	idw sum	ttr sum
Glaciers >3 km^2	750.1	1522.5	19.4	78.9	80.4	88.7	279.8	225.7	228.3	59.2	60.3	66.5
Glaciers 0.1–3 km^2	504.9	482.7	26.8	24.8	22.4	24.0	63.6	35.3	336.9	12.5	11.3	12.1
Glaciers 0.1–0.01 km^2	49.0	156.8	30.5	5.0	5.0	5.0	18.0	7.0	6.4	0.2	0.2	0.2
Glaciers >0.01 km^2	1304.1	336.4	28.6	55.1	55.1	60.5	45.3	25.6	26.1	71.9	71.9	78.9

[a]At the end of the table the totals or average values of distinct glacier size classes are shown.

glaciers larger than 3 km^2 (1 km^2) is about 15% (5%) higher with the latter interpolation. When the mean slope per glacier is directly derived from the DEM, but h_{mean} calculated with the approach by *Haeberli and Hoelzle* [1995], much smaller thickness values result for these larger glaciers, as the mean slope based on DEM cells is higher than the value from length and elevation range in these cases. On the other hand, for the smallest glaciers (h_{mean} < 30 m) the mean slope is smaller and the thickness becomes higher in GlabTop. The histogram of thickness classes in Figure 9b illustrates these differences. Most glaciers (65%–75%) have a mean ice thickness smaller than 40 m. The total volume derived from GlabTop is between 2% (using the IDW interpolation of base points) and 12% (with TopoToRaster) higher than with the *Haeberli and Hoelzle* [1995] approach.

[48] The equivalent comparison with the ITEM approach by *Farinotti et al.* [2009a] is displayed in the scatterplot of Figure 10a (R^2 = 0.69), indicating smaller mean thickness values from GlabTop, in particular for the three thickest glaciers as modeled by ITEM. These three glaciers (Aletsch, Unteraar, Rhone) are partly responsible for the 8 km^2 higher

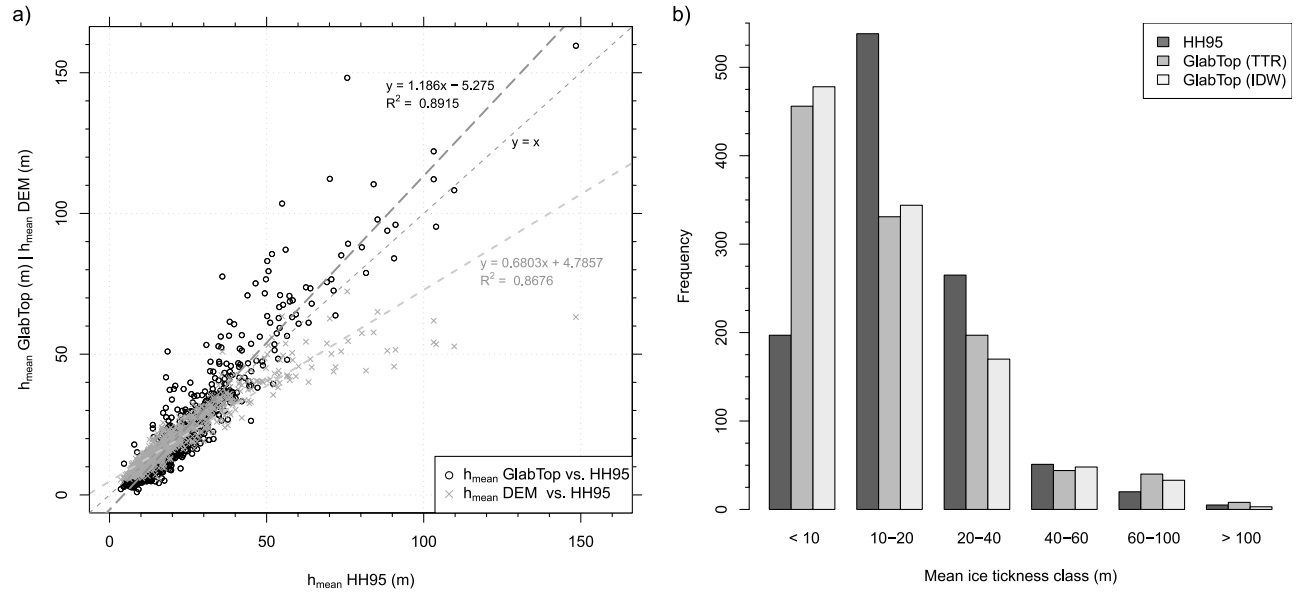

Figure 9. (a) Mean ice thickness of GlabTop and as derived from DEM-slope are displayed versus mean ice thickness derived by the approach from *Haeberli and Hoelzle* [1995]. (b) Frequency distribution of modeled mean ice thickness values.

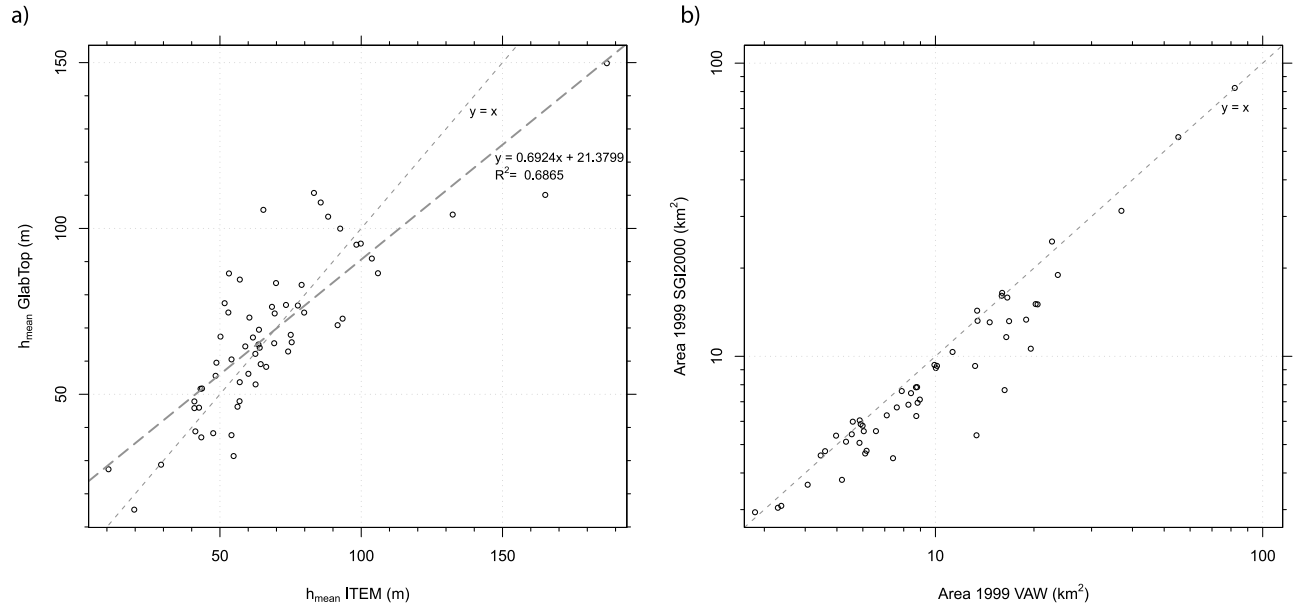

Figure 10. Comparison of GlabTop versus ITEM with (a) the mean thickness and (b) the area.

total volume of 65 ± 8 km^3 with ITEM for the year 1999 and glaciers larger than 3 km^2 compared to GlabTop. For all glaciers the difference is slightly smaller (74 ± 9 km^3 with ITEM and 68 ± 20 km^3 with GlabTop). The total volume from GlabTop for all Swiss glaciers is in this case around 10% smaller than that derived with ITEM.

8. Discussion

8.1. Ice Volume and Thickness

[49] The total ice volume for all Swiss glaciers as modeled with GlabTop (72–79 km^3 for 1973, 61–68 km^3 for 1999) is in good agreement with earlier studies by *Müller et al.* [1976] (67 km^3 for the 1970's) and *Maisch et al.* [2000] (74 km^3 for 1973), but overall 10–20% smaller than calculated with the ITEM approach by *Farinotti et al.* [2009a] (74 km^3 for 1999). The thickness and volume estimates from the different approaches nevertheless agree within the estimated general uncertainty (about 30%) with the ITEM results probably providing upper-bound values.

[50] According to our model, most glaciers smaller than 1 km^2 have mean thickness values below 20 m, or even below 10 m if they are smaller than 0.2 km^2 (cf. Figure 4b). Considering that a 10 m mean thickness translates to a maximum thickness of about 30 m (cf. section 6.1 and Figure 4a), the modeled values can still be regarded as being realistic. The more or less constant scatter in mean thickness for glaciers larger than 1 km^2, (e.g., from 50 to 100 m for glaciers with a size of 10 km^2) indicates a variability of the glacier volume by a factor of two for glaciers of the same size.

8.2. Accuracy and Uncertainties

[51] Concerning direct ice thickness measurements, GPR had started to replace earlier seismic soundings (cf., for instance *Haeberli and Fisch* [1984] and *Narod and Clarke* [1994]) and is now widely used [cf. *Farinotti*, 2010]. However, the point density of measurements per km^2 of a glacier can vary by orders of magnitude, because measurements are difficult to carry out in very steep, crevassed, avalanche- or ice-/rockfall affected areas of a glacier [*Fischer*, 2009]. For simple logistic reasons, therefore, ground-based GPR profiles mainly cover the crevasse-free flat (and thick) parts of glaciers with compressing flow (often in overdeepened parts of the bed) and might thus not be representative for the entire glacier. In order to derive the spatial distribution of ice thickness variability over entire glaciers, GPR data has therefore to be inter- and extrapolated from measured profiles using model assumptions [e.g., *Bauder et al.*, 2003; *Binder et al.*, 2009]. Smoothing techniques to reflect longitudinal stress coupling in the ice are thereby especially critical with respect to estimating thinner ice depths underneath steeper glacier parts with extending flow and intense crevasse formation: fitting models for thickness estimations to selected radar profiles is not trivial.

[52] The direct comparison with the thickness values of three glaciers shown in the GPR profiles by *Farinotti et al.* [2009b, 2009a] and *VAW* [1998] reveals that the maximum ice thickness values obtained by GlabTop are within an uncertainty range of ±30% in flat regions. For individual glaciers, ITEM gives 20–30% higher ice thickness values than GlabTop, but GlabTop can also predict higher values locally. The former largely explains the observed differences in the total glacier volume, but the area used in the ITEM model is also slightly higher (see Figure 10b). However, neither GlabTop nor ITEM is designed to resolve the glacier bed topography at a high spatial resolution. Both approaches rather allow sketching plausible bed configurations that are important to model future glacier evolution [e.g., *Jouvet et al.*, 2011]. Though absolute modeled ice thickness of places with overdeepenings have an uncertainty of ±30%, the locations of the modeled overdeepenings in the glacier bed are rather robust. To this end, the validation with the GPR profiles reveals that the locally averaged slope values of the surface topography are indeed well suited to model general glacier bed characteristics.

8.3. Glacier-Bed Topography and Future Glacier Evolution

[53] The modeled glacier beds (cf. sections 6.1 and 6.2) lead to three important implications concerning possible future glacier evolution:

[54] (i) Due to the low mean slope of the bedrock in the ablation region of the largest glaciers, a retreat of the corresponding tongues to higher elevations is hardly possible in the longer term (>50 a). As a consequence of the mass balance altitude feedback [e.g., *Raymond et al.*, 2005], such tongues cannot easily adjust their geometries to increasing temperatures, and a self-acceleration of the mass loss for surfaces located at increasingly lower elevations will occur. While this reinforcement feedback might be slowed down for some glaciers by an increasing amount of debris-cover on the surface [*Jouvet et al.*, 2011] or increased shading from adjacent slopes [*Paul*, 2010], the already observed albedo reduction (caused by small particles) might strongly enhance mass loss [*Oerlemans et al.*, 2009; *Paul et al.*, 2005].

[55] (ii) The formation of lakes in the modeled overdeepenings could strongly enhance mass loss by calving and draw-down of ice from higher areas. In contrast to current time-dependent modeling approaches [e.g., *Jouvet et al.*, 2009], the ice will probably not remain longest where the glacier ice is thickest (i.e., in the overdeepenings), but early development of pro-glacial lakes at these places may well enhance and accelerate ice loss through thermokarst effects [e.g., *Kääb and Haeberli*, 2001; *Kirkbride and Warren*, 1999] and calving processes [e.g., *Benn et al.*, 2007]. Once the ice is decoupled from the glacier it will rapidly meltdown independent of its location in a lake or on land [*Vacco et al.*, 2010], as many examples worldwide show. Due to the sedimentary characteristics of some (especially debris-covered) glaciers, shallow lakes can be filled with sediment rather than water. This aspect is a matter of further investigations, in particular in view of the potential use of such lakes for hydro-power-production, either as a reservoir or a sediment trap [*Terrier et al.*, 2011].

[56] (iii) The observation that the ice thickness in the ablation area – in particular for the largest glaciers – is often larger than in the accumulation area has important consequences for future water availability in regions with similar glacier types. After the ice in the flat and thick tongues has melted away (possibly rather fast due to reinforcement feedbacks), not much ice volume will remain in the steep back walls and summer runoff can decrease sharply in the future [*Huss et al.*, 2010]. This steep/high-altitude ice may remain there for extended times, as it is less sensitive to rising snow lines. On the other hand, medium-sized valley glaciers that have flat and thus thick accumulation regions (e.g., Trient, Giétro, Mont Miné, Ried, and Hüfi glacier) will become increasingly important with their ice reserves in terms of supplying meltwater, when most of the flat, low-altitude tongues have already disappeared.

9. Conclusions

[57] We here applied a model (named GlabTop) to obtain the ice thickness distribution for large glacier samples to the entire Swiss Alps and analyzed the characteristics of the resulting glacier beds in terms of potential future lake formation sites among others. The model provides an important alternative to mass conservation/flow models and works with limited and widely available input data (a DEM, glacier outlines and a set of central branch lines). While the uncertainty of mean thickness and volume values for unmeasured glaciers unavoidably remains high (about $\pm$30% on average) due to uncertainties in the parameterization of ice flow components, the spatial pattern of ice thickness and bed topography (including the location of overdeepenings) primarily depends on surface slope and is found to be rather robust. GlabTop provides information on a possible future (ice-free) surface topography and sites of potential lake formation, both of which are key elements for studies related to climate change impacts on landscape and glacier evolution in mountain regions [e.g., *Huss*, 2012]. The results of the here presented application of the GlabTop approach to all glaciers in the Swiss Alps reveal the following main findings:

[58] 1. While absolute values of ice thickness estimates are still affected by a relatively large uncertainty range ($\pm$30% on average and even more in individual cases), relative spatial patterns of modeled glacier-bed topography primarily depend on surface slope as contained in DEMs and are quite robust.

[59] 2. The total ice volume for all Swiss glaciers produced by GlabTop is about 75 $\pm$ 22 km^3 for 1973 and 65 $\pm$ 20 km^3 in 1999; differences to other independent estimates remain within the uncertainty range of $\pm$30%.

[60] 3. The calculated mean glacier thickness – as determined over changing glacier areas and surface elevations between 1973 and 1999 – is around 60 m.

[61] 4. When excluding the largest 15 glaciers from the sample (that contain 50% of the total volume), mean ice thickness of all other glaciers is about 40 m.

[62] 5. The modeled maximum glacier thickness is about three times larger than mean thickness (as found in earlier studies).

[63] 6. Mean thicknesses for individual glaciers of the same size vary by more than a factor of two, indicating a $\pm$50% uncertainty or even more for area-related (planar) estimates of mean glacier thicknesses or volumes.

[64] 7. The ice of the largest glaciers is often found in comparably flat/thick glacier tongues situated above weakly inclined beds at comparably low elevations (below 2300 m a.s.l.). This implies that such glaciers cannot really retreat to higher elevations with cooler conditions and may continue to shrink until the slope of the glacier bed increases substantially.

[65] 8. A considerable number of (partly large) overdeepenings is found in the modeled glacier beds; they have a total area of about 50–60 km^2 and can be seen as sites of potential future lake formation. Such lakes are of high interest for hydropower production and tourism, but they could also enhance glacier mass loss and may constitute major hazard potentials.

[66] Applicability of the model to other mountain ranges and the necessary adjustments to differing climatic, topographic and data-quality conditions must be investigated as a next step.

[67] **Acknowledgments.** This study was funded by FOEN (Federal Office of Environment) and FMV (Forces Motrices Valaisannes) as part of the two research projects CCHydro and "Climate change and hydropower." Swisstopo provided the topographic maps and DEMs used and

the VAW/ETHZ the GPR measurements for Rhone and Zinal glacier. GPR data for Corbassière glacier were kindly provided by M. Funk from VAW/ETHZ. The constructive comments of the editors A. Densmore and B. Hubbard as well as the reviews of G. Clarke and the anonymous reviewers helped to improve the manuscript considerably.

References

Bahr, D. B., M. F. Meier, and S. D. Peckham (1997), The physical basis of glacier volume-area scaling, *J. Geophys. Res.*, *102*(B9), 20,355–20,362, doi:10.1029/97JB01696.

Bauder, A., M. Funk, and G. H. Gudmundsson (2003), The ice-thickness distribution of Unteraargletscher, Switzerland, *Ann. Glaciol.*, *37*, 331–336.

Benn, D. I., C. R. Warren, and R. H. Mottram (2007), Calving processes and the dynamics of calving glaciers, *Earth Sci. Rev.*, *82*(3–4), 143–179, doi:10.1016/j.earscirev.2007.02.002.

Binder, D., E. Brückl, K. Roch, M. Behm, W. Schöner, and B. Hynek (2009), Determination of total ice volume and ice-thickness distribution of two glaciers in the Hohe Tauern region, Eastern Alps, from GPR data, *Ann. Glaciol.*, *50*, 71–79.

Chen, J., and A. Ohmura (1990), Estimation of Alpine glacier water resources and their change since the 1870s, *IAHS AISH Publ.*, *193*, 127–135.

Clarke, G. K. C., E. Berthier, C. G. Schoof, and A. H. Jarosch (2009), Neural networks applied to estimating subglacial topography and glacier volume, *J. Clim.*, *22*, 2146–2160, doi:10.1175/2008JCLI2572.1.

Driedger, C., and P. Kennard (1986), Glacier volume estimation on Cascade volcanos: An analysis and comparison with other methods, *Ann. Glaciol.*, *8*, 59–64.

ESRI (2008), *ArcGIS Desktop: Release 9.3*, Environ. Syst. Res. Inst., Redlands, Calif.

Etzelmüller, B., and H. Björnsson (2000), Map analysis techniques for glaciological applications, *Int. J. Geogr. Inf. Sci.*, *14*(6), 567–581, doi:10.1080/136588100415747.

Farinotti, D. (2010), Simple methods for inferring glacier-thickness and snow accumulation distribution, PhD thesis, Lab. of Hydraulics, Hydrol. and Glaciol. (VAW), ETH-Zurich, Zurich, Switzerland.

Farinotti, D., M. Huss, A. Bauder, and M. Funk (2009a), An estimate of the glacier ice volume in the Swiss Alps, *Global Planet. Change*, *68*(3), 225–231, doi:10.1016/j.gloplacha.2009.05.004.

Farinotti, D., M. Huss, A. Bauder, M. Funk, and M. Truffer (2009b), A method to estimate the ice volume and ice-thickness distribution of alpine glaciers, *J. Glaciol.*, *55*, 422–430.

Fischer, A. (2009), Calculation of glacier volume from sparse ice-thickness data, applied to Schaufelferner, Austria, *J. Glaciol.*, *55*, 453–460.

Frey, H., W. Haeberli, A. Linsbauer, C. Huggel, and F. Paul (2010), A multi-level strategy for anticipating future glacier lake formation and associated hazard potentials, *Nat. Hazards Earth Syst. Sci.*, *10*(2), 339–352.

Haeberli, W., and W. Fisch (1984), Electrical resistivitiy soundings of glacier beds: A test study on Grubengletscher, Wallis, Swiss Alps, *J. Glaciol.*, *30*, 373–376.

Haeberli, W., and M. Hoelzle (1995), Application of inventory data for estimating characteristics of and regional climate-change effects on mountain glaciers: A pilot study with the European Alps, *Ann. Glaciol.*, *21*, 206–212.

Haeberli, W., and J. Schweizer (1988), Rhonegletscher 1850: Eismechanische Überlegungen zu einem historischen Gletscherstand, *Mitt. VAW/ETHZ*, *94*, 59–70.

Hoelzle, M., T. Chinn, D. Stumm, F. Paul, M. Zemp, and W. Haeberli (2007), The application of glacier inventory data for estimating past climate change effects on mountain glaciers: A comparison between the European Alps and the Southern Alps of New Zealand, *Global Planet. Change*, *56*(1–2), 69–82, doi:10.1016/j.gloplacha.2006.07.001.

Huss, M. (2012), Extrapolating glacier mass balance to the mountain range scale: The European Alps 1900–2100, *Cryosphere Discuss.*, *6*(2), 1117–1156, doi:10.5194/tcd-6-1117-2012.

Huss, M., G. Jouvet, D. Farinotti, and A. Bauder (2010), Future high-mountain hydrology: A new parameterization of glacier retreat, *Hydrol. Earth Syst. Sci.*, *14*(5), 815–829.

Hutchinson, M. (1989), A new procedure for gridding elevation and stream line data with automatic removal of spurious pits, *J. Hydrol.*, *106*, 211–232, doi:10.1016/0022-1694(89)90073-5.

Jouvet, G., M. Huss, H. Blatter, M. Picasso, and J. Rappaz (2009), Numerical simulation of Rhonegletscher from 1874 to 2100, *J. Comput. Phys.*, *228*(17), 6426–6439, doi:10.1016/j.jcp.2009.05.033.

Jouvet, G., M. Huss, M. Funk, and H. Blatter (2011), Modelling the retreat of Grosser Aletschgletscher, Switzerland, in a changing climate, *J. Glaciol.*, *57*(206), 1033–1045.

Kääb, A., and W. Haeberli (2001), Evolution of a high-mountain thermokarst lake in the Swiss Alps, *Arct. Antarct. Alp. Res.*, *33*(4), 385–390.

Kamb, B., and K. A. Echelmeyer (1986), Stress-gradient coupling in glacier flow: I. Longitudinal averaging of the influence of ice thickness and surface slope, *J. Glaciol.*, *32*(111), 267–284.

Kirkbride, M. P., and C. R. Warren (1999), Tasman glacier, New Zealand: 20th-century thinning and predicted calving retreat, *Global Planet. Change*, *22*(1–4), 11–28, doi:10.1016/S0921-8181(99)00021-1.

Künzler, M., C. Huggel, A. Linsbauer, and W. Haeberli (2010), Emerging risks related to new lakes in deglaciating areas of the Alps, in *Mountain Risks: Bringing Science to Society. Proceedings of the "Mountain Risk" International Conference, 24–26 November 2010, Firenze, Italy*, edited by J.-P. Malet, T. Glade, and N. Casagli, pp. 453–458, CERG Editions, Strasbourg, France.

Laboratory of Hydraulics, Hydrology and Glaciology (VAW) (1998), Mauvoisin, Giétrogletscher, Corbassièregletscher, Glaziologische Studie im Zusammenhang mit den Stauanlagen Mauvoisin, *Tech. rep. 55.05.7903*, Lab. of Hydraulics, Hydrol. and Glaciol., ETH-Zurich, Zurich, Switzerland.

Lemke, P., et al. (2007), Observations: Changes in snow, ice and frozen ground, in *Climate Change 2007: The Physical Science Basis. Contribution of Working Group I to the Fourth Assessment Report of IPCC*, edited by S. Solomon et al., pp. 337–383, Cambridge Univ. Press, New York.

Li, H., Z. Li, M. Zhang, and W. Li (2011), An improved method based on shallow ice approximation to calculate ice thickness along flow-line and volume of mountain glaciers, *J. Earth Sci.*, *22*(4), 441–448, doi:10.1007/s12583-011-0198-1.

Li, H., F. Ng, Z. Li, D. Qin, and G. Cheng (2012), An extended "perfect-plasticity" method for estimating ice thickness along the flow line of mountain glaciers, *J. Geophys. Res.*, *117*, F01020, doi:10.1029/2011JF002104.

Linsbauer, A., F. Paul, M. Hoelzle, H. Frey, and W. Haeberli (2009), The Swiss Alps without glaciers: A GIS-based modelling approach for reconstruction of glacier beds, in *Proceedings of Geomorphometry 2009*, edited by R. Purves et al., pp. 243–247, Univ. of Zurich, Zurich, Switzerland.

Luethi, M., M. Funk, and A. Bauder (2008), Comment on 'Integrated monitoring of mountain glaciers as key indicators of global climate change: The European Alps' by Haeberli and others, *J. Glaciol.*, *54*(184), 199–200.

Maisch, M., and W. Haeberli (1982), Interpretation geometrischer Parameter von Spätglazialgletschern im Gebiet Mittelbünden, Schweizer Alpen, in *Beiträge zur Quartärforschung in der Schweiz*, pp. 111–126, Schriftenr. Phys. Geogr. Univ. Zürich, Zurich, Switzerland.

Maisch, M., A. Wipf, B. Denneler, J. Battaglia, and C. Benz (2000), Die Gletscher der Schweizer Alpen: Gletscherhochstand 1850, aktuelle Vergletscherung, Gletscherschwundszenarien, *Final rep. 31*, vdf Hochschulverlag, Zürich, Switzerland.

Marshall, S., E. White, M. Demuth, T. Bolch, R. Wheate, B. Menounos, M. Beedle, and J. Shea (2011), Glacier water resources on the eastern slopes of the Canadian Rocky Mountains, *Can. Water Resour. J.*, *36*(2), 109–134, doi:10.4296/cwrj3602823.

Müller, F., T. Caflisch, and G. Müller (1976), *Firn und Eis der Schweizer Alpen: Gletscherinventar*, Geogr. Inst. der ETH Zurich, Zurich, Switzerland.

Narod, B., and G. Clarke (1994), Miniature high-power impulse transmitter for radio-echo sounding, *J. Glaciol.*, *40*(134), 190–194.

Oerlemans, J., R. Giesen, and M. Van Den Broeke (2009), Retreating alpine glaciers: Increased melt rates due to accumulation of dust (Vadret da Morteratsch, Switzerland), *J. Glaciol.*, *55*(192), 729–736.

Paterson, W. (1994), *The Physics of Glaciers*, Pergamon, Tarrytown, N. Y.

Paul, F. (2007), The new Swiss glacier inventory 2000: Application of remote sensing and GIS, PhD thesis, Schriften. Phys. Geogr., Univ. Zürich, Zürich, Switzerland.

Paul, F. (2010), The influence of changes in glacier extent and surface elevation on modeled mass balance, *Cryosphere*, *4*(4), 569–581, doi:10.5194/tc-4-569-2010.

Paul, F., and W. Haeberli (2008), Spatial variability of glacier elevation changes in the Swiss Alps obtained from two digital elevation models, *Geophys. Res. Lett.*, *35*, L21502, doi:10.1029/2008GL034718.

Paul, F., and A. Linsbauer (2012), Modeling of glacier bed topography from glacier outlines, central branch lines and a DEM, *Int. J. Geograph. Inf. Sci.*, doi:10.1080/13658816.2011.627859, in press.

Paul, F., A. Kääb, M. Maisch, T. Kellenberger, and W. Haeberli (2004), Rapid disintegration of Alpine glaciers observed with satellite data, *Geophys. Res. Lett.*, *31*, L21402, doi:10.1029/2004GL020816.

Paul, F., H. Machguth, and A. Kääb (2005), On the impact of glacier albedo under conditions of extreme glacier melt: The summer of 2003 in the Alps, *EARSeL eProc.*, *4*(2), 139–149.

Paul, F., A. Kääb, and W. Haeberli (2007a), Recent glacier changes in the Alps observed by satellite: Consequences for future monitoring strategies,

Global Planet. Change, *56*(1–2), 111–122, doi:10.1016/j.gloplacha.2006.07.007.

Paul, F., M. Maisch, C. Rothenbuehler, M. Hoelzle, and W. Haeberli (2007b), Calculation and visualization of future glacier extent in the Swiss Alps by means of hypsographic modelling, *Global Planet. Change*, *55*(4), 343–357, doi:10.1016/j.gloplacha.2006.08.003.

Quincey, D., S. Richardson, A. Luckman, R. Lucas, J. Reynolds, M. Hambrey, and N. Glasser (2007), Early recognition of glacial lake hazards in the Himalaya using remote sensing datasets, *Global Planet. Change*, *56*(1–2), 137–152, doi:10.1016/j.gloplacha.2006.07.013.

Radic, V., and R. Hock (2010), Regional and global volumes of glaciers derived from statistical upscaling of glacier inventory data, *J. Geophys. Res.*, *115*, F01010, doi:10.1029/2009JF001373.

Raper, S. C. B., and R. J. Braithwaite (2009), Glacier volume response time and its links to climate and topography based on a conceptual model of glacier hypsometry, *Cryosphere*, *3*(2), 183–194.

Raymond, C., T. A. Neumann, E. Rignot, K. Echelmeyer, A. Rivera, and G. Casassa (2005), Retreat of Glaciar Tyndall, Patagonia, over the last half-century, *J. Glaciol.*, *51*(173), 239–247.

Rickenbacher, M. (1998), Die digitale Modellierung des Hochgebirges im DHM25 des Bundesamtes für Topographie, *Wiener Schr. Geograph. Kartographie*, *11*, 49–55.

Rothenbühler, C. (2006), GISALP: Räumlich-zeitliche Modellierung der klimasensitiven Hochgebirgslandschaft des Oberengadins, PhD thesis, Geograph. Inst., Univ. Zürich, Zürich, Switzerland.

Swiss Federal Office of Topography (2005), Das digitale Höhenmodell der Schweiz, report, Bundesamt für Landestopographie, Wabern, Switzerland.

Terrier, S., F. Jordan, A. Schleiss, W. Haeberli, C. Huggel, and M. Künzler (2011), Optimized and adapted hydropower management considering glacier shrinkage scenarios in the Swiss Alps, in *Proceedings of the International Symposium on Dams and Reservoirs under Changing Challenges: 79th Annual Meeting of ICOLD, Swiss Committee on Dams, Lucerne, Switzerland*, edited by A. Schleiss and R. Boes, pp. 497–508, Taylor and Francis, London.

Vacco, D. A., R. B. Alley, D. Pollard, and D. B. Reusch (2010), Numerical modeling of valley glacier stagnation as a paleoclimatic indicator, *Quat. Res.*, *73*(2), 403–409, doi:10.1016/j.yqres.2009.09.006.

Watson, R., and W. Haeberli (2004), Environmental threats, mitigation strategies and high-mountain areas, *Ambio*, *13*, 2–10.

World Glacier Monitoring Service (WGMS) (2008), Global glacier changes: Facts and figures, report, U. N. Environ. Prog., Zurich, Switzerland.

Zemp, M., A. Kääb, M. Hoelzle, and W. Haeberli (2005), GIS-based modelling of glacial sediment balance, *Z. Geomorphol.*, *138*, 113–129.

Zemp, M., et al. (2007), *UNEP: Global Outlook for Ice and Snow*, pp. 115–152, U. N. Environ. Prog., Nairobi.